Erosion of Poly(anhydride-co-imides): A Preliminary Mechanistic Study

J. O. SEIDEL, K. E. UHRICH,* C. T. LAURENCIN,† and R. LANGER‡

Department of Chemical Engineering, Massachusetts Institute of Technology, Cambridge, Massachusetts 02139

SYNOPSIS

A new class of biodegradable polymers that show promising characteristics for orthopedic applications was investigated. This study examines aspects underlying the polymer erosion of poly[trimellitylimidoglycine-co-1,6-bis(carboxyphenoxy)hexane] and poly[pyromellitylimidoalanine-co-1,6-bis(carboxyphenoxy)hexane]. Copolymer degradation was studied by examining the anhydride bond hydrolysis and copolymer composition by IR and NMR spectroscopy. Hydrolysis of the anhydride bonds occurred much faster than did the dissolution of the hydrolyzed products, leading to the formation of two distinct erosion zones. The two erosion zones were observed by light and scanning electron microscopy with erosion originating at the surface and moving to the center of the polymer samples. © 1996 John Wiley & Sons, Inc.

INTRODUCTION

Surface-eroding materials, such as polyanhydrides,[1] display erosion characteristics that include a pattern of material loss from outside to inside and a rate of erosion that is dependent on the surface area of the polymer matrix, in contrast to the bulk-eroding polyesters which display material loss throughout the polymer matrix and a rate dependence on the polymer matrix volume.[2,3] Degradation of surface-eroding polymers is therefore characterized by a gradual overall decrease in polymer implant size. This erosion pattern may provide opportunities for tissue ingrowth into the device and allow for the preservation of the polymer matrix molecular weight and mechanical strength within the uneroded portions of the polymer.

Poly(anhydride-co-imides) matrices are novel biodegradable polymeric materials with good me-

chanical properties designed specifically for orthopedic applications.[4] They were designed to combine the desirable surface-eroding characteristics of the polyanhydrides with the excellent mechanical properties of polyimides. Amino acids were used as building blocks, linked via hydrolytically unstable anhydride bonds at their carboxy terminus and mechanically strong imide linkages at their amino terminus.[4] Because of their good mechanical properties and excellent biocompatibility characteristics, they are being investigated for use in bone repair and drug delivery.[4-6] To assess the suitability of these materials for long-term orthopedic applications, tissue biocompatibility of the poly(anhydride-co-imides) has been evaluated. Tissue responses to the poly(anhydride-co-imides) matrices were mild and appeared qualitatively equivalent to the initial response to poly(lactic-co-glycolic acid) (PLGA) matrices used as the control.[7] They did, however, not show a sudden release of degradation products that can potentially lead to tissue irritation as was previously observed for PLGA matrices.[2,3,8]

Degradation of these poly(anhydride-co-imides) occurred via hydrolysis of anhydride bonds, followed by hydrolysis of imide bonds and dissolution of the monomer units.[9,10] The linear degradation profiles of discs, along with linear release kinetics of incorporated small molecular weight drugs, strongly sug-
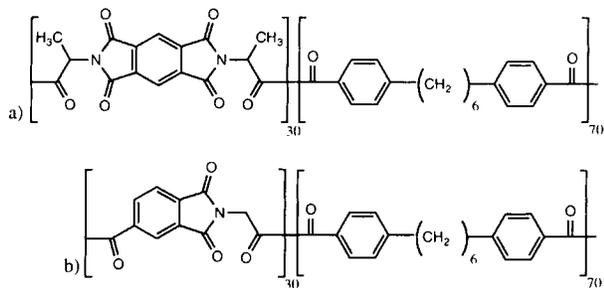
Figure 1 Structure of (a) PMA-ala : CPH (30 : 70) and (b) TMA-gly : CPH (30 : 70).

gests that this novel family of bioerodible polymers are surface eroding.[11] These degradation studies focused on the dissolved polymer degradation products and the release of the incorporated small molecules.

This study examines the erosion and degradation mechanism of poly[trimellitylimidoglycine-co-1,6-bis(carboxyphenoxy)hexane], with a molar ratio of 30 : 70 as denoted by TMA-gly : CPH (30 : 70) [Fig. 1(a)] as well as poly[pyromellitylimidoalanine-co-1,6-bis(carboxyphenoxy)hexane], with a molar ratio of 30 : 70 as denoted by PMA-ala : CPH (30 : 70) [Fig. 1(b)]. Extensive physicochemical analysis of the eroding polymer, such as light and electron microscopy, as well as IR and NMR spectroscopy were used to provide additional insight into the nature of polymer matrix erosion and degradation of poly(anhydride-co-imides).

MATERIALS AND METHODS

Polymer Synthesis

TMA-gly : CPH (30 : 70) and PMA-ala : CPH (30 : 70) were polymerized by an anhydride-exchange melt polymerization as described elsewhere.[4,12] TMA-gly : CPH (30 : 70) had a weight-average molecular weight (M_w) of 6600 with a polydispersity index (PDI) of 2.3 and PMA-ala : CPH (30 : 70) had an M_w of 5300 with a PDI of 1.7. Molecular weights were determined on a Perkin-Elmer system consisting of an isocratic LC pump 250 and LC-30 RI detector. Turbochem3 software was used on a DECpc 433 data station for data analysis. Samples dissolved in chloroform were eluted through two columns in series (Polymer Laboratories, PL-Gel, linear and 100 Å). Molecular weights of the polymers were determined relative to narrow molecular weight polystyrene standards (Polysciences).

Sample Preparation

Polymer cylinders were prepared by compression molding. The polymer powder (average weight of 1.01 ± 0.02 g) was placed in an 8 mm-diameter cylindrical die and pressed with a Carver Press (Fred S. Carver, Inc., Wabash, IN) with a 3800-4000 lb load for 10 min. The PMA-ala : CPH cylinders were pressed at room temperature. The TMA-gly : CPH cylinders were pressed at 37 ± 3°C to avoid crack formation when the cylinder was extracted from the die. Cylinder height-to-diameter ratio was 2 : 1. The pressed cylinders had a homogeneous brown color (relative to the original light orange-brown colored powder) and a smooth surface.

In Vitro Degradation

The polymer cylinders were placed in scintillation vials containing 15 mL of $0.1 M$ phosphate buffer at pH 7.4 and incubated at 37°C. The phosphate buffer was changed frequently (every 4 h for the first 2 days, every 12 h for the next 5 days, every day for 1 week, and then every 2 days for the remainder of the study) to approximate perfect sink conditions, as determined by previous studies.[10] The buffer solution containing the degradation products was decanted from the polymer cylinder and fresh solution added to the vial. The polymer cylinders were analyzed at 0, 1, 3, 8, 21, and 35 days. All experiments were done in triplicate.

Microscopy

Cross sections of the fractured samples were examined under a light microscope (Wild Macroscope M420) with no special preparation necessary. The observed erosion zones were also examined by scanning electron microscopy (SEM). Cross sections were vacuum-dried, mounted, sputtered with 400 Å of gold, and examined by SEM using a Stereoscan 250 MK3 microscope from Cambridge Instruments (Cambridge, MA) at 20 kV.
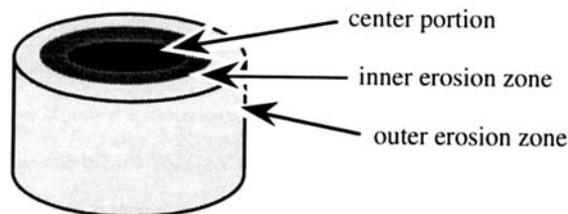
Figure 2 Different erosion zones illustrated on a cross section of the polymer cylinder.
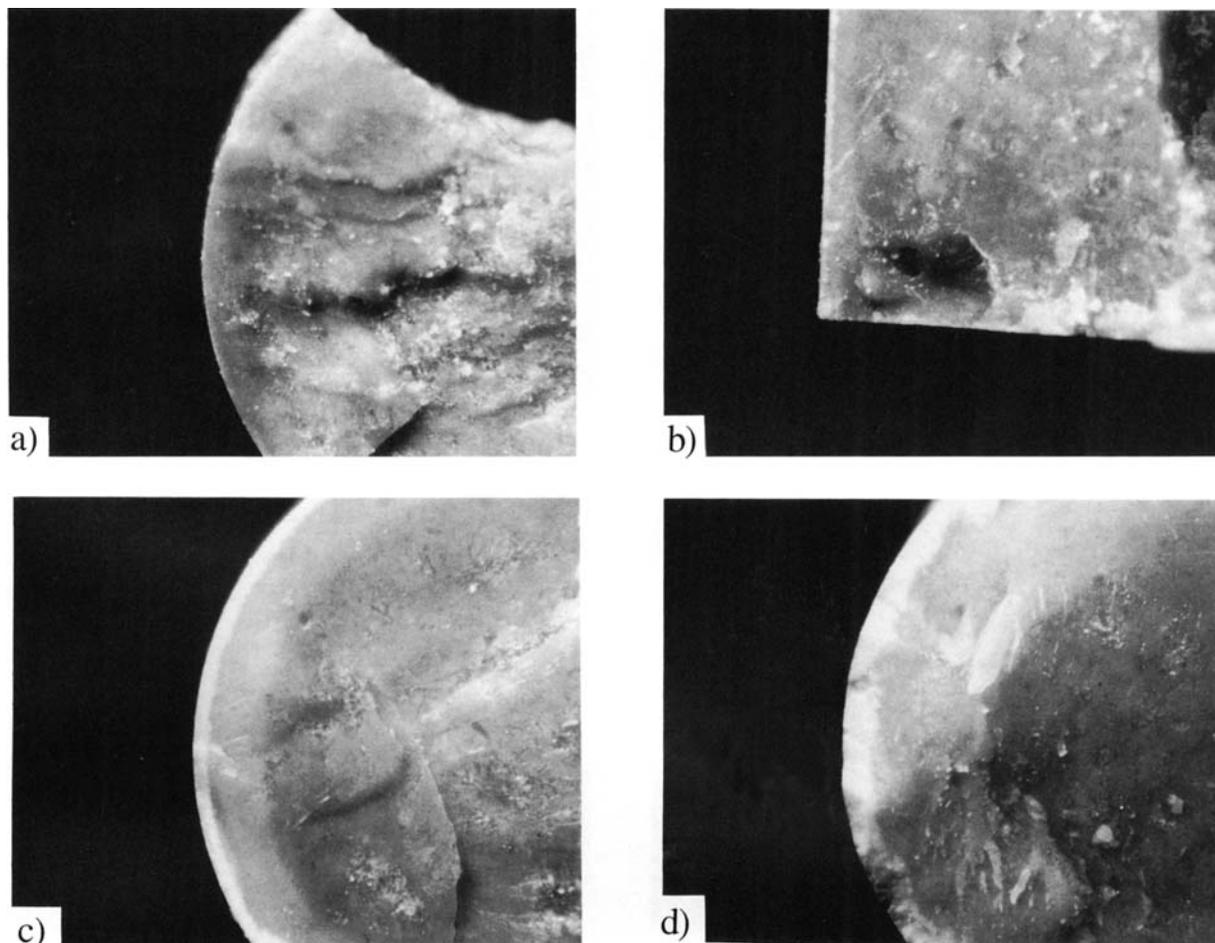
Figure 3 Erosion zones as seen by light microscope (Magnification 22×) for PMA-ala : CPH samples, after 1 (3a), 3 (3b), 7 (3c) and 21 days (3d) of erosion in 0.1M phosphate buffer solution (pH 7.4) at 37°C. The dark bar on the top of the pictures indicates the noneroded polymer; the light bar indicates the inner erosion zone and the spotted bar indicates the outer erosion zone.

Chemical Analysis

The degraded cylinders of the two copolymers, PMA-ala : CPH (30 : 70) and TMA-gly : CPH (30 : 70), were analyzed by several methods. The different erosion zones (Fig. 2) were first separated by scraping with a scalpel under the light microscope. The outer layer (outer erosion zone) had a very light beige color and was easily removed. The area between the outer erosion zone and the innermost portion of the degraded sample (inner erosion zone) showed a light brown color and was more difficult to remove than was the outer erosion zone. The removed material was then mixed with a mortar and pestle and pressed into KBr pellets for IR spectroscopy or dissolved in d_7-DMF for ^{1}H-NMR spectroscopy.

Infrared spectroscopy data was obtained on a Nicolet Magna 550 FTIR spectrometer and Nicolet

data station with OMNIC 1.20 software. Samples were pressed into KBr pellets to determine the amount of hydrolysis of the polymer and monomer chains. The characteristic absorbance frequencies for the aliphatic and aromatic anhydride bonds were 1800–1850 and 1760–1800 cm^{-1}, respectively; the aliphatic and aromatic acid groups resonated at 1760–1800 and 1600–1700 cm^{-1}, respectively; and the C — C bonds of the aromatic ring resonated at 1560–1620 cm^{-1}. To quantitate the decrease in the anhydride absorbance, the aliphatic anhydride region and the C — C bond region of the aromatic rings in the IR spectra were analyzed by determining the total absorbance in those regions and comparing them to a reference absorbance. The aryl C — C stretch was chosen as an internal reference as this frequency should not be affected by hydrolysis. The number of aromatic rings was assumed to be con-
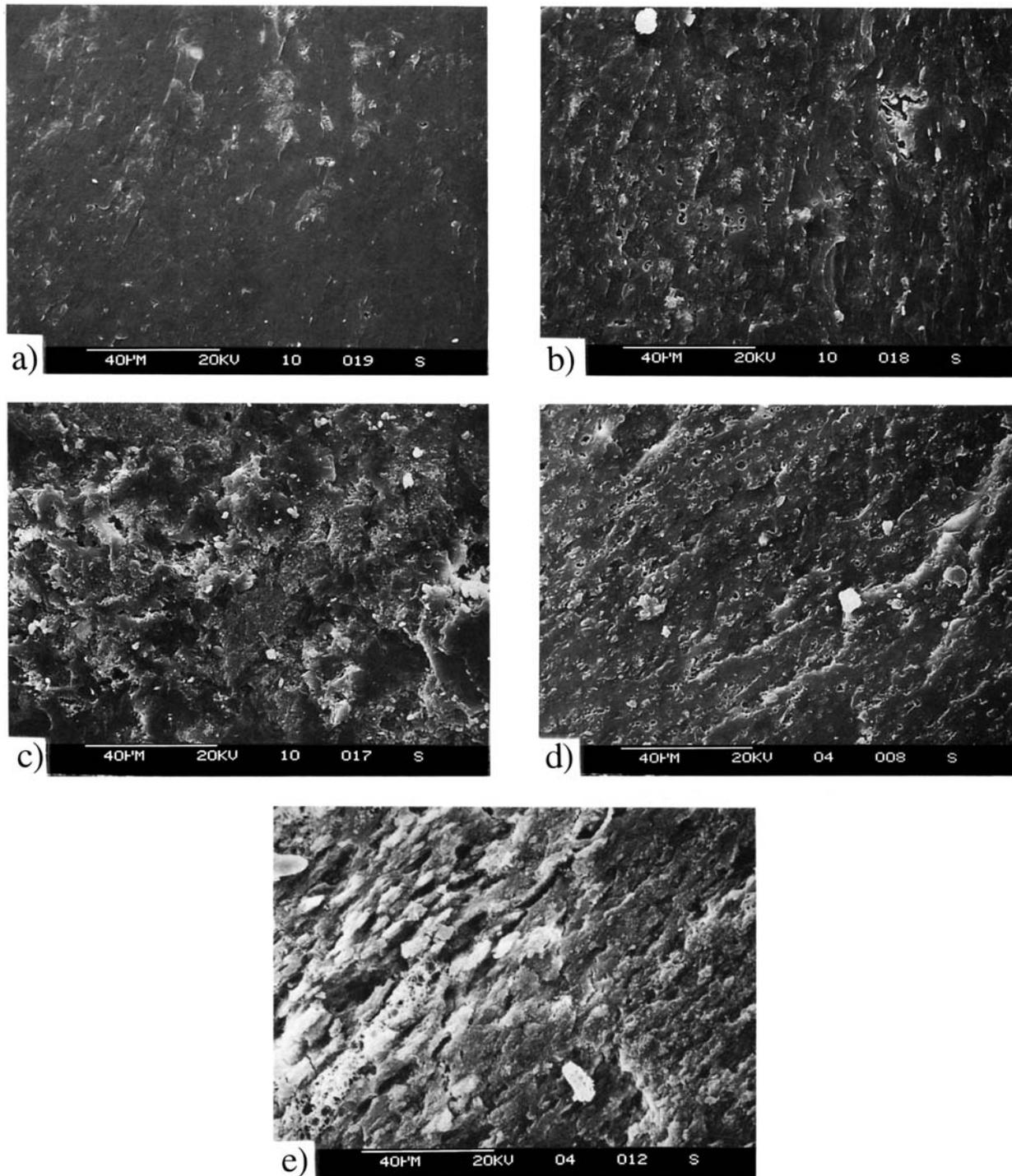
Figure 4   SEM micrographs (Magnification 700×) of the different zones after 8 days of degradation in 0.1M phosphate buffer solution (pH 7.4) at 37°C. The center of the PMA-ala : CPH sample (4a) shows a small number of pores with a diameter of less than 5 μm. The inner erosion zone (4b) showed an increase in pore size (5–10 μm) and number. Figure 4c shows the outer erosion zone of the PMA-ala : CPH sample with pore size up to 15 μm and some pores connecting to form a connected pore system. TMA-gly : CPH samples show a higher porosity in the inner (4d) as well as the outer erosion zone (4e), even though there was no apparent difference in the initial porosity. The pore size in the outer zone ranges up to 20 μm and most pores are connected to form an open pore system.
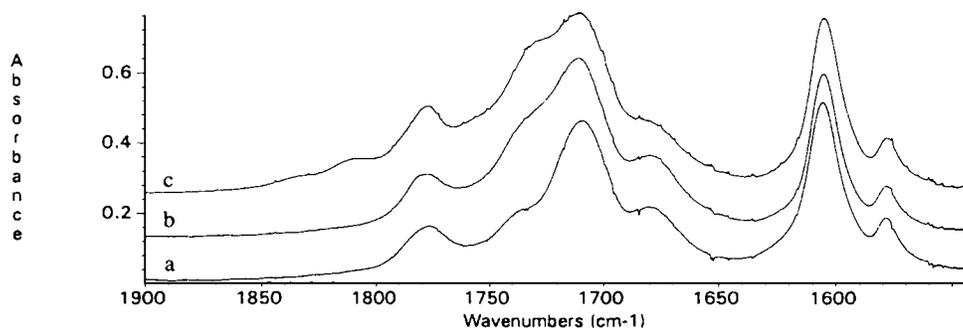
Figure 5   IR spectra of PMA-ala : CPH after three weeks of degradation: (a) the outer erosion zone, (b) the inner erosion zone and (c) the center of the sample.

stant relative to the number of anhydride or acid functional groups. Thus, the ratio of aliphatic anhydride absorbencies to the aryl C — C ring stretch for each spectra was reported.

^{1}H-NMR spectra of the three zones of the cylinders were obtained on a Nicolet 360 MHz spectrometer on solutions in d_7-DMF using the solvent as reference to determine the anhydride : imide ratio of the different polymer erosion regions. The ratio was calculated from the integral ratio of the methine protons of the PMA-ala at 5.2–5.3 ppm relative to the methylene protons of the CPH at 3.9–4.3 ppm. For TMA-gly : CPH, the methylene protons of TMA-gly at 4.5–4.8 ppm were measured relative to the methylene protons of the CPH (3.9–4.3 ppm).

For solubility studies, an excess of each monomer was suspended in 10 mL of 0.1 M phosphate buffer at pH 5, 7.4, or 10. The solutions were stored at 37°C for 60 min, then at room temperature for at

least 48 h. Heating over longer periods of times hydrolyzed the imide bonds of PMA-ala. The samples were filtered through 0.25 μm pore-size filters, then assayed with a Perkin-Elmer UV/vis spectrophotometer (Model Lambda 3B) at 248 nm. A calibration curve was generated for each monomer.[10]

RESULTS AND DISCUSSION

Erosion Zones

The cylinders were fractured and the fractured pieces were investigated by light microscopy. The fractured surfaces were generally parallel to the cylinder ends. For both types of copolymers, two erosion fronts (an inner and an outer zone) were observed during the study (Fig. 3). This is in contrast to findings with other polyanhydride copolymers, where only one erosion zone was observed.[3,13] Similar
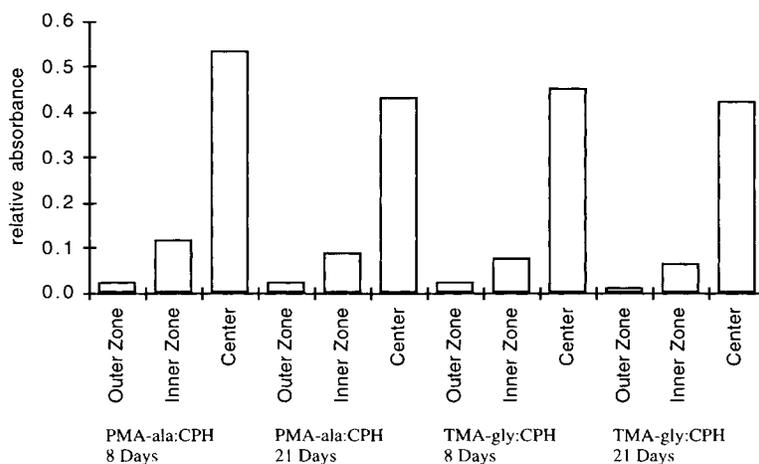
Figure 6   Changes in the relative intensity of the aliphatic anhydride IR absorbance (1800–1850 cm^{-1}) with respect to the aromatic ring absorbance in the different zones for the two poly(anhydride-*co*-imides) at 8 and 21 days.
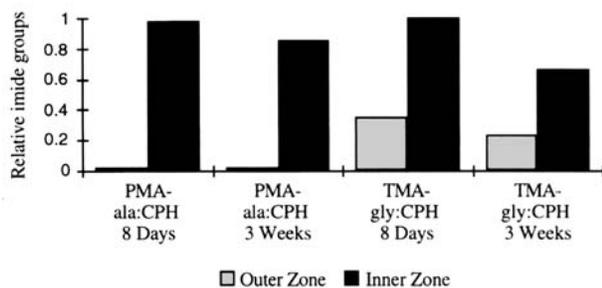
Figure 7 Relative amount of imide content of the polymer for the two erosion zones relative to the center portion (undegraded).

to the earlier studies, it could be seen that the zones extended further and further into the interior core of the sample, moving from the surface to the inside, as the time in aqueous solution increased. These observations suggest that the poly(anhydride-co-imides) have surface-eroding characteristics similar to polyanhydrides. This article examines the mechanisms responsible for the formation of these two visible erosion zones.

After 1 day in aqueous media, degradation of the PMA-ala : CPH device had turned the surface lighter in color and an erosion zone had proceeded only slightly into the sample [Fig. 3(a)]. After 3, 7, and 21 days, two distinct zones could be seen [Fig. 3(b)–(d)]. The same two zones could be observed for the TMA-gly : CPH samples. After only 1 day, the cylinder surface had turned very light in color, indicating that erosion had started. After 3 days, a clear distinction between the inner and the outer erosion zone could be made, similar to Figure 3(b). With the prolonged exposure to the degradation media, the zones moved further toward the center of the sample.

Examination of the polymer cylinders by SEM showed that the undergraded PMA-ala : CPH sample had a small number of pores with a diameter of less than 5 microns. The pores were likely produced during compression molding of the polymer. No differences in porosity could be observed between an undegraded polymer cylinder and the center of the PMA-ala : CPH cylinders degraded for 8 days [Fig. 4(a)]. The inner erosion zone in the PMA-ala : CPH cylinders showed an increase in pore size (5–10 μm) and number [Fig. 4(b)]. The outer erosion zone [Fig. 4(c)] presented a further increase in pore number and size (10–15 μm), and the pores were connected. The structure of this system allowed the surrounding aqueous media to penetrate and form channels between the pores. Polymer degradation products

could then diffuse through these newly formed channels.

The morphologies described for the different zones in the PMA-ala : CPH copolymer devices were also observed in the TMA-gly : CPH copolymer cylinders. The center of the TMA-gly : CPH samples after 8 days of degradation showed the same size pores as those of the undegraded polymer samples. The inner erosion zones of the TMA-gly : CPH copolymer showed more and bigger pores [Fig. 4(d)] than did the corresponding PMA-ala : CPH sample [Fig. 4(b)] at a similar degradation time (8 days). The outer erosion zones of the TMA-gly : CPH copolymer also had bigger pores than did the PMA-ala : CPH samples (up to 20 μm) with more open connections between the pores [Fig. 4(e)]. Light microscopy and SEM analysis showed that significant erosion of the polymer matrix occurred in the outer erosion zone and that no detectable erosion can be seen in the center of the polymer samples.

Chemical Analysis

Infrared spectra of the center of the cylinders of the two different copolymers (degraded for 8 and 21 days) are similar to the spectra of the undegraded polymer samples, indicating that there has not been any detectable hydrolysis of the polymer in the center of the samples during this period. Comparison of the IR spectra of the three zones (center, inner erosion, outer erosion) after 21 days showed a clear decrease in the anhydride absorbance due to hydrolysis of the anhydride and imide bonds on the surface of the sample relative to the undegraded polymer sample interior (Fig. 5). Hydrolysis occurred to a significant extent in both the inner and outer erosion zones. A decrease in the ratio of aliphatic anhydride absorbencies (1800–1850 cm^{-1}) relative to the aryl C — C ring stretches showed a decrease in the number of aliphatic anhydride bonds with respect to the number of aromatic rings (Fig. 6). For all of the degraded samples, the anhydride : aryl ring ratio was much lower in the inner and outer erosion zones

Table I   Monomer solubility [moles/L].

Monomer	pH 7.4
TMA	3.45×10^{-1}
TMA-gly	6.49×10^{-2}
PMA	5.76×10^{-2}
PMA-ala	5.09×10^{-2}
CPH	$<10^{-5}$

than in the center portion, indicating that a significant number of anhydride bonds were hydrolyzed in these two erosion zones. The remaining absorbance of the CPH–CPH anhydride bonds after 3 weeks indicates that the outer erosion zone still contained slowly degrading CPH–CPH bonds.

^{1}H-NMR spectra revealed the composition of the erosion zones by determining the anhydride-to-imide ratio of the copolymer. The change in composition was significant, especially in the outer erosion zone. Figure 7 shows the relative decrease of the imide component of the polymer for the two erosion zones relative to the center (undegraded portion) of the sample.

The NMR data indicated that the imide monomer component of the copolymer (PMA-ala or TMA-gly) was removed from the polymer cylinder faster than was the other monomer, CPH. No PMA-ala was found in the outer erosion zone of the PMA-ala : CPH samples after only 8 days, whereas some TMA-gly was still detected in the outer zone of the TMA-gly : CPH copolymers after 3 weeks. This may be attributed to the higher hydrophilicity of the PMA-ala : CPH copolymer matrices relative to TMA-gly : CPH matrices.[4] The more rapid release of the more hydrophilic comonomer was also observed by Tamada and Langer.[3] It was concluded that the differences in the degradation rates of the anhydride bonds connected to the two different monomer units affected the erosion of the polyanhydride copolymers.

In summary, the erosion mechanism of poly-(anhydride-*co*-imides) was defined by microscopic and spectroscopic techniques. The combined data from microscopy, IR, and ^{1}H-NMR spectra indicated that the erosion of the polymer happened in several steps. After absorption of water into the polymer matrix, hydrolysis of the anhydride bonds occurred at the forefront of the inner erosion zone, as judged by IR spectroscopy. Hydrolysis of the polymer backbone continued until monomer units were solubilized in water. Water absorption and hydrolysis of the anhydride bonds occurred simultaneously as shown by Shieh et al.[13] Finally, the monomer units were removed by diffusion through the polymer matrix and only the CPH monomer remained in the device due to the lower reactivity of the CPH–CPH anhydride bond and the low water solubility of the CPH (Table I).[10]

REFERENCES

1. L. Shieh, A. Göpferich, and R. Langer, *Mater. Res. Soc. Symp. Proc.,* **331**, 85–90 (1994).
2. S. Li, H. Garreau, and M. Vert, *J. Mater. Sci. Mater. Med.,* **1**, 123–130 (1990).
3. J. A. Tamada and R. Langer, *Proc. Natl. Acad. Sci. U.S.A.* **90**, 552–556 (1993).
4. K. U. Uhrich, A. Gupta, T. T. Thomas, C. K. Laurencin, and R. Langer, *Macromolecules,* **28**(7), 2184–2193 (1995).
5. M. A. Attawia, K. E. Uhrich, E. Botchwey, M. Fan, C. T. Laurencin, and R. Langer, *J. Biomed. Mat. Res.,* to appear.
6. M. A. Attawia, K. E. Uhrich, E. Botchwey, R. Langer, and C. T. Laurencin, *J. Orthop. Res.,* to appear.
7. S. E. M. Ibim, K. E. Uhrich, R. Brunston, R. Langer, and C. T. Laurencin, to appear.
8. O. M. Böstman, *J. Bone Joint Surg.,* **73**, 148–153 (1991).
9. K. U. Uhrich, T. T. Thomas, C. K. Laurencin, and R. Langer, to appear.
10. K. U. Uhrich, D. R. Larrier, C. K. Laurencin, and R. Langer, *J. Polym. Sci.,* to appear.
11. S. E. M. Ibim, K. U. Uhrich, M. E. P. Goad, A. Chen, R. Huang, C. T. Laurencin, to appear.
12. A. Staubli, E. Ron, and R. Langer, *J. Am. Chem. Soc.,* **112**, 4419–4424 (1990).
13. L. Shieh, J. Tamada, I. Chen, J. Pang, A. Domb, and R. Langer, *J. Biomed. Mater. Res.,* **28**, 1465–1475 (1994).